Ion evaporation from the surface of a Taylor cone

F. J. Higuera
ETS Ingenieros Aeronáuticos, Plaza Cardenal Cisneros 3, 28040 Madrid, Spain
(Received 5 February 2003; published 14 July 2003)

An analysis is carried out of the electric field-induced evaporation of ions from the surface of a polar liquid that is being electrosprayed in a vacuum. The high-field cone-to-jet transition region of the electrospray, where ion evaporation occurs, is studied taking advantage of its small size and neglecting the inertia of the liquid and the space charge around the liquid. Evaporated ions and charged drops coexist in a range of flow rates, which is investigated numerically. The structure of the cone-to-jet transition comprises: a hydrodynamic region where the nearly equipotential surface of the liquid departs from a Taylor cone and becomes a jet; a slender region where the radius of the jet decreases and the electric field increases while the pressure and the viscous stress balance the electric stress at the surface; the ion evaporation region of high, nearly constant field; and a charged, continuously strained jet that will eventually break into drops. Estimates of the ion and drop contributions to the total, conduction-limited current show that the first of these contributions dominates for small flow rates, while most of the mass is still carried by the drops.

DOI: 10.1103/PhysRevE.68.016304 PACS number(s): 47.15.Gf, 47.65.+a

I. INTRODUCTION

Electrostatic atomization is a technique for generating sprays of monodisperse drops of electrically conducting liquids with diameters ranging from micrometers to nanometers. It is used, for example, in mass spectrometry, electric propulsion, food and pharmaceutical industries, and electrostatic deposition. In a basic configuration, the liquid to be electrosprayed is fed through a capillary needle and forms a meniscus at the end of the needle. A voltage difference is applied between the needle and an opposite electrode (extractor) to create a field around the liquid which brings electric charge to its surface and elongates the meniscus in the direction of the field. In certain ranges of voltage and liquid flow rate, the meniscus takes the form of a cone whose tip emits a thin jet that breaks into electrically charged drops at some distance from the meniscus. This is the so-called cone-jet mode in the classification introduced by Cloupeau and Prunet-Foch [1]. The hydrostatic balance of surface tension and electric stress which leads to a conical meniscus was ascertained by Taylor [2]. Analyses of the electrohydrodynamics of the cone-jet and discussions of the extensive work carried out in this area can be found in Refs. [3–6], among others.

Ions may accompany the charged drops of an electrospray. Field-enhanced evaporation of ions has long been known to occur at the surface of a metallic liquid and finds application in liquid metal ion sources (LMIS) [7]. More recently, Iribarne and Thomson [8] proposed that the same phenomenon might be responsible for the evaporation of ions dissolved in dielectric liquids, and Fenn *et al.* [9] used it to explain the generation of ions from tiny drops of solutions of large, fragile biomolecules in electrospray ionization. Though the idea of field-enhanced evaporation from dielectric liquids was not immediately accepted, it has received first indirect support [10–12] and then direct confirmation by Gamero-Castaño and Fernández de la Mora [13] and Gamero-Castaño [14], who measured the current of emitted ions. Working with electrosprays of concentrated solutions of NaI in formamide and other liquids in a vacuum, these authors find that electric fields of the order of 1 V/nm, which are required to evaporate ions from these liquids, can be realized both in the largest drops generated immediately upon the breakup of the jet and in the cone-to-jet transition region of the meniscus. According to their scaling laws and those of Fernández de la Mora and Loscertales [3], the maximum electric field should be proportional to the power 1/6 of the ratio of the electrical conductivity of the liquid to the flow rate injected through the meniscus. Their experiments with liquids of conductivities of the order of 1 S/m and above demonstrate that ion evaporation appears in the predicted regions when the flow rate Q is sufficiently small. They find a regime of coexistence of ions and drops in which the total electric current stays above the well-known $I \propto Q^{1/2}$ law for regular electrosprays, reaches a minimum, and then increases with decreasing Q. Romero *et al.* [15], in further experiments with the ionic liquid $EMIBF_4$, find that the drop emission vanishes entirely for flow rates close to the smallest flow rate at which a Taylor cone can be established, leaving a regime of pure ionic emission akin to that of LMIS.

Beams of charged drops and ions have long been used for electric propulsion. Early research in the 1960s centered much on highly stressed electrosprays of glycerol electrolytes, chosen for its high dielectric constant and small volatility, but handicapped by a small electrical conductivity that limits the charge-to-mass ratio of the drops and thus the specific impulse attainable at reasonable acceleration voltages; see Martínez-Sánchez *et al.* [16] for a detailed account. More recent research has been prompted by the requirements of new space applications such as microsatellites and formation flying missions that depend on a controllable thrust in the range of tens of micronewtons. Gamero-Castaño and Hruby [17] and Bocanegra *et al.* [18] discuss the possibilities offered by new propellants such as formamide seeded with ammonium salts, tributyl phosphate, and ionic liquids to meet the opposite, mission-dependent requirements imposed on the specific impulse, the energy per unit thrust and the propulsion efficiency.

This paper is devoted to an analysis of the evaporation of ions from the cone-to-jet transition region of an electrospray in the regime in which a jet is left beyond the ion evaporation region. This jet will eventually break into a spray of charged drops that coexist with the ions in some downstream region, but neither these processes nor the feeding needle and the meniscus upstream of the transition region need to be analyzed in detail if use is made of the disparity of scales between the tiny transition region and all the other regions. Numerical simulations and order-of-magnitude estimates are used to characterize the flow and ion evaporation in the cone-to-jet transition region. Estimates are derived for the ions and drops electric currents and for the range of flow rates where the ions-and-drops regime can be realized.

II. FORMULATION

Ion emission by field-induced evaporation from the surface of a polar liquid in a vacuum is well described by Iribarne and Thomson [8] mechanism, which (for liquids of large dielectric constant and surfaces of small curvature [10]) is embodied in the expression

$$j_e = \frac{kT}{h}\sigma \exp\left[-\frac{\Delta G - G_E(E)}{kT}\right],$$

$$\text{with} \quad G_E(E) = \left(\frac{e^3 E}{4\pi\epsilon_0}\right)^{1/2}, \tag{1}$$

giving the electric current density across the surface j_e as a function of the surface density of free charge σ and the electric field E at the surface of the liquid. Here k and h are the Boltzmann and Planck constants, e is the elementary charge, ϵ_0 is the permittivity of vacuum, T is the temperature, and ΔG is the activation energy for ion evaporation in the absence of an electric field. Typical values of the ratio $\Delta G/kT$ for liquids that undergo ion evaporation are in the range of 50–100 at ambient temperature. This means that the rate of evaporation is negligible in the absence of an electric field, and also that the exponential factor in Eq. (1) changes from very small to very large when the field increases through a narrow range of width $2kTE^*/\Delta G$ around a value of the order of $E^* = 4\pi\epsilon_0(\Delta G)^2/e^3$, which makes the exponent equal to zero. Typical values of E^* are of the order of 1–2 V/nm.

The mass flux across the liquid surface accompanying the evaporation current is

$$\phi_e = \zeta j_e, \tag{2}$$

where ζ is the mass-to-charge ratio of the solvated ions that evaporate.

Electric fields of the order of E^* may be attained in the electrospraying of a sufficiently conducting liquid in a vacuum. In the absence of ion evaporation, the electric field at the surface of the liquid has a maximum in the cone-to-jet transition region. This maximum field increases, and the size of the transition region decreases, when the flow rate is decreased or the electrical conductivity of the liquid is increased [3–6]. Typical values of the radius of the jet when the electric field reaches values of the order of E^* in the experiments of Gamero-Castaño *et al.* [13,14] and Romero *et al.* [15] are about 10 nm, and the required flow rates are in the range of 10^{-14}–10^{-13} m^3/s. Estimates of the density of space charge around the evaporation region of the surface based on the measured evaporation current and electric fields of the order of E^* suggest that the field induced by the space charge can be neglected at small evaporation currents, so that the electric potential in the vacuum around the liquid ($-\varphi$ with $\boldsymbol{E} = \boldsymbol{\nabla}\varphi$) satisfies $\nabla^2\varphi = 0$.

The small values of the flow rate and the size of the cone-to-jet transition region where evaporation occurs bring in important simplifications to the analysis.

On one hand, the structure of the flow in the cone-to-jet transition region becomes independent of the configuration of the needle holding the meniscus and of the extractor. This is because the transition region is small compared with any other length of the system. Consider the meniscus upstream of the transition region. The velocity and the electric field in the liquid decrease rapidly upstream of the transition region, so that only surface tension and normal electric stress are important in the balance of stresses that determines the shape of the surface. Leaving out the effect of the space charge and advancing that the effect of the charge of the jet far downstream is also negligible [see Eq. (14) below], this balance of stresses yields the classic Taylor equipotential cone [2] of semiangle $\alpha = 49.29°$, for which $\varphi = \varphi_T(R,\theta) = BR^{1/2}P_{1/2}(\cos\theta)$. Here $P_{1/2}$ is Legendre's function of degree 1/2, R is the distance to the apex of the cone, θ is the angle around the apex, measured from the prolongation of the cone axis, and

$$B = \frac{2^{1/2}}{-P'_{1/2}(-\cos\alpha)\sin\alpha(\tan\alpha)^{1/2}}\left(\frac{\gamma}{\epsilon_0}\right)^{1/2}$$

$$= 1.3459\ldots\left(\frac{\gamma}{\epsilon_0}\right)^{1/2}.$$

Taylor solution provides thus the far field asymptotics for the cone-to-jet transition region.

On the other hand, the Reynolds number based on the flow rate and the size of the transition region is moderate or small, which suggests that the inertia of the liquid does not play an important role in this region. The pressure variations and viscous stresses estimated with these same magnitudes are of the order of the surface tension and electric stress in the transition region. This is at variance with known estimates for the cusp of a LMIS [7,19], for which typical values of the surface tension and the electric field are ten times larger than in the present case, leading to curvature radii of the surface ten times smaller, and the flow rates are so small that flow-induced stresses at the surface are always small compared with surface tension and electric stresses.

Neglecting the inertia of the liquid altogether, the flow in the transition region and the electric potentials in the liquid and in the vacuum obey Stokes and Laplace equations, respectively. Boundary conditions at the surface express, in the context of the leaky dielectric model [20], the balances of

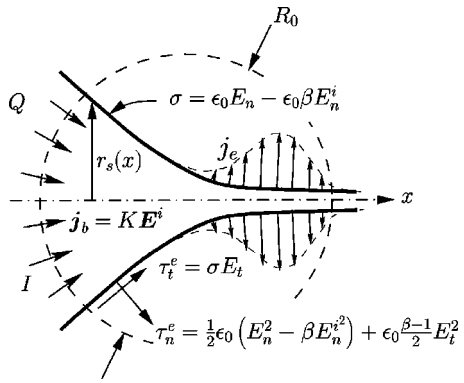

FIG. 1. Definition sketch.

mass and momentum, the continuity of the electric potential, and a transport equation for the free surface charge, whose density determines the jump of the component of the electric displacement normal to the surface. Figure 1 is a sketch of the transition region. Inspection shows that the problem to be solved in this region contains the following parameters: the viscosity μ, electrical conductivity K, surface tension γ, and dielectric constant β of the liquid; the permittivity of vacuum ϵ_0; the flow rate Q injected through the meniscus; and the constants entering the evaporation law (1) and (2). Scales for the different magnitudes involved can be built from the first three of these parameters plus the permittivity of vacuum using dimensional analysis. They are

$$R_0=\frac{\epsilon_0\gamma}{\mu K},\quad v_0=\frac{\gamma}{\mu},\quad E_0=\frac{\mu^{1/2}K^{1/2}}{\epsilon_0},$$

$$Q_0=v_0R_0^2,\quad I_0=KE_0R_0^2, \tag{3}$$

$$\varphi_0=E_0R_0,\quad \sigma_0=\epsilon_0E_0.$$

Using these scales to nondimensionalize the problem, and denoting the nondimensional variables with the same symbols used before for their dimensional counterparts, we are led to the following formulation:

$$\left.\begin{aligned}&\nabla\cdot\boldsymbol{v}=0\\&0=-\nabla p+\nabla^2\boldsymbol{v}\\&\nabla^2\varphi^i=0\end{aligned}\right\}\quad \text{for}\quad r<r_s(x), \tag{4}$$

$$\nabla^2\varphi=0\quad \text{for}\quad r>r_s(x), \tag{5}$$

where x and r are cylindrical coordinates (see Fig. 1), $r=r_s(x)$ is the surface of the liquid, which occupies the region $r<r_s(x)$, $\boldsymbol{v}$ and p are the liquid velocity and pressure, and φ^i and φ are the negative of the electric potentials in the liquid and in the vacuum, respectively, so that $\boldsymbol{E}^i=\nabla\varphi^i$ and $\boldsymbol{E}=\nabla\varphi$ are the electric fields.

The boundary conditions are the following:

$$\nabla\cdot\boldsymbol{n}=p-\boldsymbol{n}\cdot\tau'\cdot\boldsymbol{n}+\frac{1}{2}(E_n^2-\beta E_n^{i^2})+\frac{1}{2}(\beta-1)E_t^2, \tag{6}$$

$$\boldsymbol{t}\cdot\tau'\cdot\boldsymbol{n}=\sigma E_t, \tag{7}$$

$$\frac{dI_s}{dx}=2\pi r_s(E_n^i-j_e)(1+r_s'^2)^{1/2}, \tag{8}$$

$$\text{with}\quad I_s=2\pi r_s v\sigma\quad\text{and}\quad j_e=\sigma\exp[A(E^{1/2}-E^{*1/2})],$$

$$\boldsymbol{v}\cdot\boldsymbol{n}=\zeta j_e,\quad \sigma=E_n-\beta E_n^i,\quad E_t=E_t^i \tag{9}$$

at the surface $r=r_s(x)$;

$$\varphi^i=\frac{I}{2\pi(1-\cos\alpha)R},$$

$$\text{with}\quad I=I_s+I_b\quad\text{and}\quad I_b=2\pi\int_0^{r_s}E_x^i r\,dr, \tag{10}$$

$$\psi=-\frac{BP'_{1/2}(-\cos\alpha)}{2\pi(1-\cos\alpha)}IR^{1/2}f_B(-\cos\theta)$$

$$+\frac{Q}{2\pi(1-\cos\alpha)}(1+\cos\theta), \tag{11}$$

$$\omega\to 0 \tag{12}$$

in the liquid far upstream, for $x\to-\infty$ and $r<r_s(x)\sim -x\tan\alpha+o(1)$, where ψ and ω are the stream function and the vorticity, and the origin of coordinates is at the apex of the cone;

$$r_s=O\left(\frac{\tilde{Q}}{\tilde{I}x^{1/2}}\right),\quad v=O\left(\frac{\tilde{I}^2x}{\tilde{Q}}\right),$$

$$\sigma=O\left(\frac{1}{x^{1/2}}\right),\quad p=O\left(\frac{\tilde{I}x^{1/2}}{\tilde{Q}}\right),$$

$$\text{with}\quad \tilde{I}=I-I_e(\infty),\quad \tilde{Q}=Q-\zeta I_e(\infty),$$

$$\text{and}\quad I_e(\infty)=2\pi\int_{-\infty}^{\infty}j_e(1+r_s'^2)^{1/2}r_s\,dx, \tag{13}$$

in the liquid far downstream, for $x\to\infty$; and

$$\varphi=\varphi_T(R,\theta)+O\left(\frac{\tilde{Q}}{\tilde{I}R}\right),$$

$$\text{with}\quad \varphi_T=BR^{1/2}P_{1/2}(\cos\theta),\quad B=1.3459\ldots, \tag{14}$$

in the vacuum for $(x,r)\to\infty$.

Here $R=\sqrt{x^2+r^2}$ and $\theta=\arctan r/x$ are spherical coordinates; $\boldsymbol{n}=(-r_s',1)/\sqrt{1+r_s'^2}$ and $\boldsymbol{t}=(1,r_s')/\sqrt{1+r_s'^2}$ are unit vectors normal and tangent to the surface, respectively; $E_n=\boldsymbol{E}\cdot\boldsymbol{n}$ and $E_t=\boldsymbol{E}\cdot\boldsymbol{t}$, and similarly for the electric field in the liquid; $\tau'=\frac{1}{2}[\nabla\boldsymbol{v}+(\nabla\boldsymbol{v})^T]$ is the viscous stress tensor; I_s and I_b are the surface convection and bulk conduction currents, respectively; j_e is the current density of ions evaporating from the surface nondimensionalized with KE_0, so that $I_e(\infty)$ in Eq. (13) is the total nondimensional current evapo-

rated from the cone-to-jet transition region and $\tilde{I}$ is the current left in the downstream jet; and finally, the mass-to-charge ratio of the evaporating ions ζ has been nondimensionalized with $\rho Q_0/I_0$, where ρ is the density of the liquid. The total flow rate evaporated in the transition region is ζI_e, and $\tilde{Q}$ is the part of the injected flow rate Q that is left in the downstream jet.

Equation (6) is the balance of stresses normal to the surface. The left-hand side is the surface tension stress and the last two terms on the right-hand side are the normal electric stress [20,21]. The flux of momentum carried by the evaporating ions is neglected. Equation (7) is the balance of stresses tangent to the surface, the right-hand side being the electric shear stress. Equation (8) is the balance of free charge at the surface. The free surface charge is convected by the flow, leading to an electric current that increases due to the conduction current reaching the surface from the liquid and decreases due to the evaporation of ions. Conditions (9) express the proportionality of the flow rate and electric current crossing the surface, and the electrostatic conditions that the jump of the normal component of the electric displacement across the surface is equal to the surface density of free charge and that the component of the electric field tangent to the surface is continuous.

Far upstream of the evaporation region, the meniscus tends to a Taylor cone where the field normal to the surface and the density of free surface charge are proportional to $1/R^{1/2}$. The surface current tends to zero for $R\to\infty$ due to the decrease of the surface charge and the velocity of the liquid, and the evaporation current also decreases very rapidly as the electric field decreases. Thus, only conduction in the liquid is left to transport the electric current in this far region, which is the cause of the radial variation of the electric potential in Eq. (10). The radial field in the liquid and the free charge at the surface lead to an electric shear that induces a recirculating flow whose stream function is given by the first term of Eq. (11), with $f_B(\xi)$ solving $(1-\xi^2)(f_B^{iv}-4\xi f_B'''+\frac{3}{2}f_B'')-\frac{15}{16}f_B=0$, $f_B(1)=f_B(\cos\alpha)=f_B''(\cos\alpha)+1=0$, and $f_B'(1)<\infty$; see Ref. [22]. The second term of Eq. (11) is the stream function of the sink flow due to the flow rate Q injected through the meniscus.

The asymptotic conditions (13) in the jet downstream of the evaporation region come from the order of magnitude balances

$$v r_s^2 \sim \tilde{Q}, \quad \sigma v r_s \sim \tilde{I}, \quad p \sim \frac{1}{r_s},$$

$$\frac{p r_s^2}{x} \sim \sigma E_t r_s, \quad E_t \sim \frac{1}{x^{1/2}}, \tag{15}$$

which express the conservation of the flow rate and the electric current which have not evaporated (conduction is negligible in the far jet because the cross section and the electric field decrease with streamwise distance), the balance of pressure and surface tension, the axial increase of the pressure due to the electric shear at the surface, and the condition that the axial field in this far downstream region is induced by the surface charge in the conical meniscus far upstream, decreasing as in Taylor solution [2].

Finally, Eq. (14) gives the electric potential in the vacuum away from the evaporation region as that of Taylor solution plus a correction due to the surface charge in the jet far downstream.

Problem (4)–(14) contains the properties of the liquid lumped in the four nondimensional parameters

$$\beta, \quad \zeta, \quad A, \quad \text{and} \quad E^*, \tag{16}$$

where

$$A=\frac{(e^3E_0/4\pi\epsilon_0)^{1/2}}{kT} \quad \text{and} \quad E^*=\frac{4\pi\epsilon_0(\widehat{\Delta G})^2}{e^3E_0}$$

$$\text{with} \quad \widehat{\Delta G}=\Delta G-kT\ln\left(\frac{kT}{h}\frac{\epsilon_0}{K}\right).$$

Its solution should determine the flow and the electric fields, the surface of the liquid, and the electric currents that evaporate and are left in the jet in terms of these parameters and the nondimensional flow rate Q injected through the meniscus.

The scaling factors (3) depend only on physical properties of the liquid and the permittivity of vacuum ϵ_0, but not on the flow rate, which can be varied independently of the liquid, nor the parameters appearing in the evaporation law (1) and (2). Alternative scaling factors have been used in Refs. [3,13] which are based on K, γ, ϵ_0, and the flow rate instead of μ. The relations between the current and the viscosity nondimensionalized with these factors ($\hat{I}$ and $\hat{\mu}$ say) and the nondimensional current and flow rate used here are $\hat{I}=I/Q^{1/2}$ and $\hat{\mu}=Q^{1/3}$. (The nondimensional variables used in Ref. [3] are actually $\beta^{1/2}\hat{I}$ and $\beta^{2/3}/\hat{\mu}$.) Similarly, the alternative nondimensional maximum electric field at the surface and the corresponding radius of the surface are $\hat{E}_M=E_MQ^{1/6}$ and $\hat{r}_M=r_M/Q^{1/3}$, where E_M and r_M are the values of these magnitudes nondimensionalized with E_0 and R_0 in Eq. (3). Dimensional analysis shows that, in the absence of inertia and ion evaporation,

$$\hat{I}=f_1(\hat{\mu},\beta), \quad \hat{E}_M=f_2(\hat{\mu},\beta), \quad \hat{r}_M=f_3(\hat{\mu},\beta). \tag{17}$$

In addition, it has been observed experimentally that the viscosity of the liquid is not an important parameter in determining the current and other properties of the solution. If the solution was strictly independent of $\hat{\mu}$, then Eq. (17) would imply that $\hat{I}$, $\hat{E}_M$, and $\hat{r}_M$ are constant for a given liquid [3,13]. The current would then be strictly proportional to the square root of the flow rate; the maximum electric field would be inversely proportional to the sixth root of the flow rate; and the size of the cone-to-jet transition region would be of the order of the charge relaxation length [3]: $(\epsilon_0\beta/K)^{1/3}\times(\text{flow rate})^{1/3}$. Bringing out these results is the main merit of the nondimensionalization that leads to Eq. (17). On the other hand, qualitative order-of-magnitude esti-

mates aimed at describing a consistent structure of the solution have been worked out in Ref. [6] and in Sec. III B below. These estimates suggest that the proportionality of the electric current and the square root of the flow rate is realized when $1 \ll Q \ll \beta^2$, but the solution develops then a multiscale structure in which the maximum electric field is not attained in the charge relaxation region but in a somewhat smaller region immediately downstream of it, where the appropriate scale of the field differs slightly from the one derived from Eq. (17) with the assumption of $\hat{\mu}$ independence. This result, if it is correct, brings in a weak dependence of the solution on the viscosity of the liquid.

III. RESULTS

A. Numerical solutions

The parameter A measures the sensitivity of the evaporation current j_e in Eq. (8) with the electric field. It is typically large. Values for formamide and $EMIBF_4$ at ambient temperature are 112.91 and 221.92, respectively, with E_0 in (3) evaluated for a conductivity $K=1$ S/m. In these conditions $E^*=0.4$ and 0.12, respectively. Values of E^* are somewhat larger for other liquids that do not undergo evaporation in a Taylor cone. This has been rationalized [13,15] noticing that (i) there is a minimum flow rate below which a cone jet cannot be established in the absence of evaporation [3,13], and (ii) the field at the surface increases when the flow rate decreases. Therefore, the minimum flow rate determines the maximum attainable field and, given the strong sensitivity of j_e with the electric field, evaporation will be negligible if this maximum field is smaller than E^*.

The large values of A make up for a difficult numerical problem. Numerical solutions of (4)–(14) have been computed here for values of A smaller than in real experiments, in the hope that this will not induce qualitative changes in the problem. A similar approach has been often taken in combustion problems also involving high activation energies [23], for which comparison with asymptotic results is sometimes possible and supports this kind of approximation, at least for stationary solutions.

The electric current is plotted in Fig. 2 as a function of the flow rate for $A=60$ and an otherwise realistic set of parameter values. The solid curve gives the total current and the dash-and-dot curve gives the current $\tilde{I}$ left in the jet. The dashed curve is the I–Q relation for the same values of the parameters but in the absence of ion evaporation (j_e set equal to zero); it displays the well-known behavior $I \propto Q^{1/2}$ [3,4,6]. The total current departs from the square root law when Q decreases, though the divergence of the solid and dashed curves in Fig. 2 is less pronounced than in the experiments of Gamero-Castaño and Fernández de la Mora [13] because of the reduced value of A used here. The total current is always larger than the current in the absence of evaporation, while the current left in the jet is smaller than this reference current because evaporation decreases somewhat the surface charge density. The numerical method fails to converge below a certain value of Q at which the evaporation current is already considerably larger than $\tilde{I}$. The current in

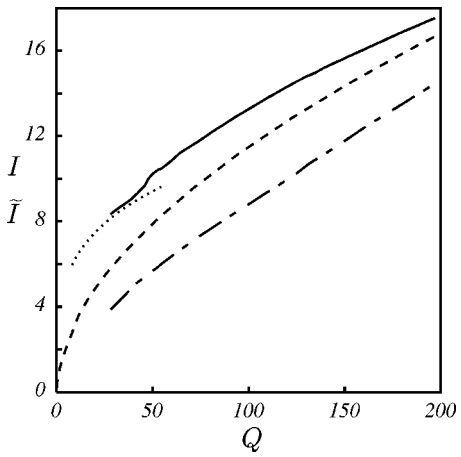

FIG. 2. Total electric current (I, solid), current left in the jet ($\tilde{I}$, chain), and electric current in the absence of ion evaporation (dashed), as functions of the flow rate for $\beta=50$, $\zeta=0$, $A=60$, and $E^*=0.36$. The dotted line at the left is $I=3.54\,Q^{1/4}$.

Fig. 2 displays a small hump for Q about 50, which does not exist when $E^*=0.49$ (not shown). In some of the cases of Fig. 3, for other values of the parameters, the hump has developed into a minimum and a maximum of the current. This kind of response is in line with the experimental results of Romero *et al.* [15], though the extrema are shallower here than in their experiments and the value $\beta=5$ is not the representative of the polar liquids for which evaporation has been observed. (Large values of the dielectric constant β are needed to achieve large electrical conductivities and thus large electric fields; cf. the expression of E^* below Eq. (16) with E_0 in (3) proportional to $K^{1/2}$.)

The streamwise evolution of the different components of the electric current is shown in Fig. 4 for a sample case. The electric field at the surface and the surface charge density are given in Fig. 5. The bulk conduction current [I_b defined in Eq. (10)] dominates in the meniscus, decreases monotoni-

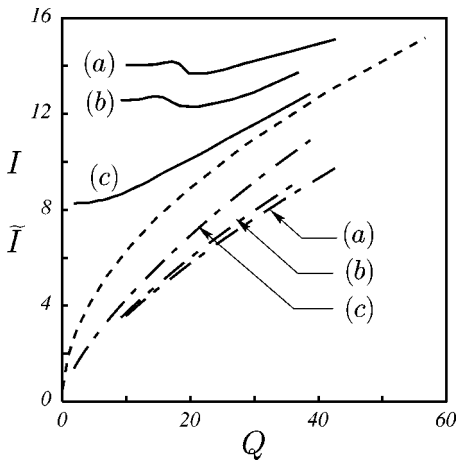

FIG. 3. Total electric current (I, solid), current left in the jet ($\tilde{I}$, chain), and electric current in the absence of ion evaporation (dashed), as functions of the flow rate for $\beta=5$, $\zeta=0$, and the couples of values (a): $(A,E^*)=(50,0.4225)$; (b): (60,0.4225); and (c): (50,0.49).

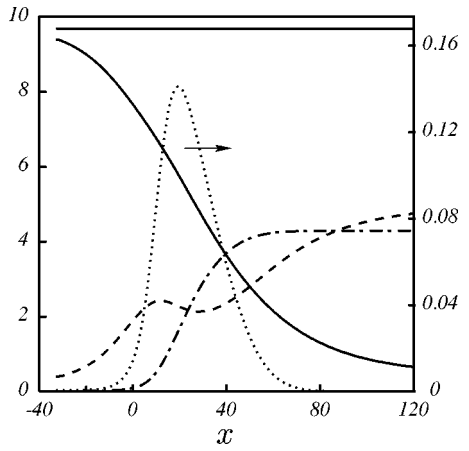

FIG. 4. Conduction current (I_b, solid), convection current (I_s, dashed), accumulated evaporation current (I_e, chain), and evaporation current density ($2\pi r_s j_e$, dotted, right side scale), as functions of the axial distance, for $Q=46$, $\beta=50$, $\zeta=0$, $A=60$, and $E^*=0.36$. The upper horizontal line gives the total current $I=I_b+I_s+I_e$.

cally through the transition region, and tends to zero in the jet far downstream, where $I_b \sim \tilde{Q}^2/(\tilde{I}^2 x^{3/2})$ when Eqs. (13) and (15) are used. The surface current [I_s in Eq. (8)] first increases, as the component of $\boldsymbol{E}^i$ normal to the surface carries conduction current to the surface, then goes through a maximum and a minimum in the evaporation region, where the surface charge density also has a minimum, and finally increases towards its asymptotic value $\tilde{I}$ in the jet, where the surface charge density keeps decreasing [see Eqs. (13) and Fig. 5] due to the continuous straining of the jet by the electric shear at its surface. Ion evaporation is concentrated around the maximum of the electric field; the evaporation current $2\pi r_s j_e$, with j_e in Eq. (8), decreases rapidly at both sides of the maximum. The accumulated evaporation current $I_e(x)=2\pi\int_{-\infty}^{x} j_e \sqrt{1+r_s'^2}\, r_s\, dx$ rises from zero to a constant value, and the total current $I=I_b(x)+I_s(x)+I_e(x)$ is a constant.

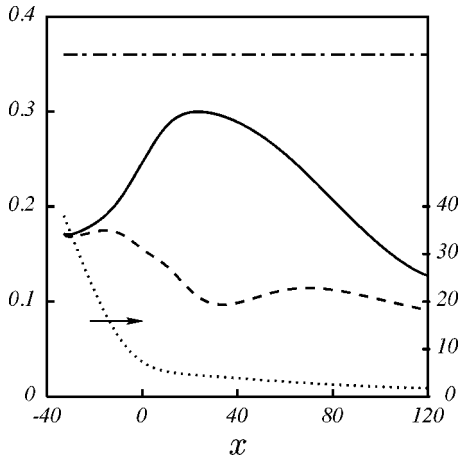

FIG. 5. Electric field at the outer side of the surface (E_n, solid), surface charge density (σ, dashed), and radius of the surface (r_s, dotted, right side scale), as functions of the axial distance, for $Q=46$, $\beta=50$, $\zeta=0$, $A=60$, and $E^*=0.36$ (upper horizontal line).

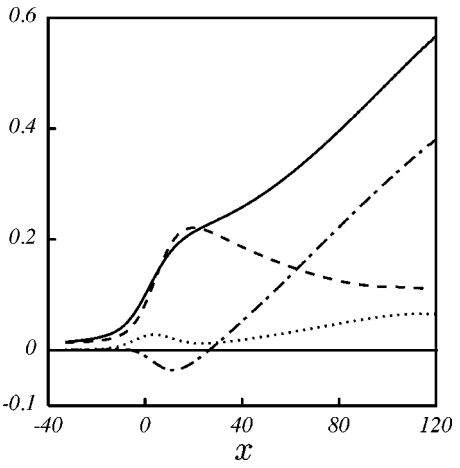

FIG. 6. Surface tension (solid), normal electric stress (dashed), pressure (chain), and normal viscous stress (dotted), as functions of the axial distance, for $Q=46$, $\beta=50$, $\zeta=0$, $A=60$, and $E^*=0.36$.

The stresses normal to the surface are shown in Fig. 6. The pressure and normal viscous stress are negligible in the meniscus far upstream, where the balance of surface tension and normal electric stress which is characteristic of Taylor hydrostatic solution prevails. In the jet far downstream, on the other hand, the normal electric stress becomes negligible and there is a balance of surface tension and pressure, as it has been advanced in the estimates (15) that led to the downstream asymptotic conditions (13). In between, the pressure goes through a minimum, taking negative values, and the normal electric stress goes through a maximum before decreasing in the jet.

B. Asymptotic estimates

This section describes qualitative features of the solution of (4)–(14) in the formal limit $(Q,\beta)\gg 1$, $E^*\ll 1$, $A\gg 1$.

1. Evaporation onset

Ion evaporation is negligible until the maximum electric field at the surface rises to make $A[\max(E)^{1/2}-E^{*1/2}]=O(1)$ in Eq. (8). An evaporation onset can be defined in the asymptotic limit $A\to\infty$ by the condition

$$\max(E)=E^*, \tag{18}$$

where the maximum field is evaluated in the absence of evaporation, being therefore a function of Q and β only. Gamero-Castaño *et al.* [13,14] and Romero *et al.* [15] have used this condition along with $\max(E)=f(\beta)/Q^{1/6}$ and $f(\beta)$ determined experimentally. This law was first proposed by Fernández de la Mora and Loscertales [3] on the basis of a model in which the maximum field is attained in a region of characteristic size $(\beta Q)^{1/3}$ around the apparent apex of the conical meniscus where the residence time of the flow is of the order of the electrical relaxation time of the liquid [$R/v=O(\beta)$ with $v=O(Q/R^2)$, in nondimensional variables]; see the discussion at the end of Secs. II and III B 2 below. The same result has been derived [13] by patching the elec-

tric fields around the cone and around the jet. Carrying this expression of max(E) to Eq. (18) gives a critical flow rate Q^* proportional to $1/E^{*6}$ above which evaporation is negligible. This is in qualitative agreement with experimental results.

Asymptotic estimates for large values of Q and β [6] suggest, however, that the maximum field is attained in the rear part of the cone-to-jet transition region, already in the jet, and scales as $1/Q^{1/8}$ when $Q \gg \beta^4$ and as $\beta^{1/2}/Q^{1/4}$ when $Q \ll \beta^4$. Though these asymptotic results might be realized only for very large values of Q and β, they can be used in Eq. (18) to give, in their ranges of validity,

$$\left.\begin{aligned} Q^* &= O(1/E^{*8}) \quad \text{for } \beta^{1/2}E^* \ll 1 \\ Q^* &= O(\beta^2/E^{*4}) \quad \text{for } \beta^{1/2}E^* \gg 1 \end{aligned}\right\} \tag{19}$$

at the onset of ion evaporation.

The asymptotic estimates leading to these results are extended below to cases of vigorous evaporation for flow rates below Q^*, assuming that a stationary solution still exists in the evaporation region and around.

2. Hydrodynamic region

The recirculating flow induced by the electric shear at the surface of the cone [the first term of Eq. (11)] dominates for $R \gg (Q/I)^2$, which are very large distances in the conditions of interest here. The radial sink flow represented by the second term of Eq. (11) dominates for smaller values of R, in an intermediate region where the surface is still a cone. This radial flow is an exact irrotational solution of the Stokes equations in a cone, with no associated pressure variations or viscous stresses at the surface. Pressure variations and viscous stresses should appear in the region where the surface deflects away from a cone. The characteristic velocity of the liquid in this hydrodynamic region is $v_h = Q/R_h^2$, and its size R_h is determined by the condition that the nondimensional pressure and normal viscous stress, of $O(v_h/R_h)$, should become of the order of the surface tension and normal electric stress in Taylor solution, of $O(1/R_h)$. Thus, $R_h = O(Q^{1/2})$ and $v_h = O(1)$, whereas $E_n = O(Q^{-1/4})$ at the outer side of the surface. The liquid is screened from this field by the electric charge at the surface.

On the other hand, the density of free surface charge σ leads to a surface current of the order of $\sigma v R$ in the meniscus, whose streamwise variation requires a field $E_n^i = O(\sigma v/R)$ in the liquid in order for electric conduction to carry the appropriate additional charge to the surface [the estimate of E_n^i comes from the balance of dI_s/dx and the right-hand side of Eq. (8) without ion evaporation]. This is admissible while $\beta E_n^i \lesssim E_n$ in the second condition (9), which, with $\sigma = O(E_n)$ from this same condition, amounts to $R/v \gtrsim \beta$; i.e., a residence time of the order of the electrical relaxation time or larger. The condition $R/v = O(\beta)$ defines the electric relaxation region of Fernández de la Mora and Loscertales [3], of size $R_e = O(\beta Q)^{1/3}$, where $E_n = O(\beta Q)^{-1/6}$.

This relaxation region comes out smaller than the hydrodynamic region when $Q \gg \beta^2$, so that the estimate of R_e is not applicable in this case and the free surface charge adjusts almost instantaneously to make the surface of the liquid an equipotential down to $R = O(R_h)$ and in at least a certain stretch of the jet. In the opposite case when $Q \ll \beta^2$, surface charge relaxation ceases to be possible before the pressure and normal viscous stress become sufficiently strong to deform the surface. Then the density of free surface charge cannot increase at the pace of E_n for $R \ll R_e$, as would be required to screen the liquid. The second condition (9) simplifies to $\beta E_n^i \approx E_n$ and the current freezes at a value of the order of the characteristic surface current in the relaxation region, $Q^{1/2}/\beta^{1/2}$, in agreement with Ref. [3]. Even in these conditions, however, the electric field in the liquid is small compared with E_n when $\beta \gg 1$ (an inner field of the order of E_n in the electric relaxation region would lead to a conduction current of the order of $\beta^{1/2}Q^{1/2}$, larger than the current observed in the absence of evaporation [3]). It is the polarization charge rather than the free surface charge that prevents such high fields from entering the liquid. This case of $Q \ll \beta^2$ will not be realized in the estimates that follow, but it could be relevant to the pure ionic regime of Romero *et al.* [15].

3. Slender jet

The following two conditions should hold in the leading part of the jet downstream of the hydrodynamic region.

First, the surface of the jet should be nearly equipotential. This is a condition of matching with the hydrodynamic region upstream. Should the electric field enter the liquid immediately upon the surface becoming a slender jet, this field would originate a conduction current that is too large and whose streamwise variation could not be balanced by the variation of the surface current. The condition of a nearly equipotential surface also underlies the analyses of the cusp region of a LMIS upstream of the cap where ion evaporation occurs [24]. The jet lies on the prolongation of the cone, where the axial field induced by the charge at the surface of the cone is of the order of $Q^{-1/4}$ at distances of the order of R_h from its apparent apex and decreases as $1/x^{1/2}$ further downstream [from Eq. (14)]. This field is to be balanced by the field of the charge at the surface of the jet, which acts as a line distribution of charge. In terms of the radius of the jet, $r_s(x)$, and the field normal to its surface, $E_n(x)$, the axial component of the field induced by the line distribution of charge is $d(E_n r_s)/dx$ up to logarithms (see e.g., Ref. [25]). The condition that this field should balance the axial field of the meniscus is, in orders of magnitude,

$$\frac{E_n r_s}{x} \sim \frac{1}{x^{1/2}}. \tag{20}$$

Second, the pressure and normal viscous stress of the liquid on the surface should balance the normal electric stress. The normal viscous stress is of the order of $\partial v_r/\partial r = O(\partial v/\partial x)$, from the continuity equation, where v_r and v are the radial and axial components of the velocity. Pressure

variations along the jet should be of the same order as the normal viscous stress, in the presence of vorticity generated at the surface. With $v=O(Q/r_s^2)$, the order-of-magnitude balance of these stresses and the normal electric stress reads

$$\frac{Q}{xr_s^2}\sim E_n^2. \tag{21}$$

Conditions (20) and (21) imply $x=O(Q^{1/2})$ and $E_n=O(Q^{1/4}/r_s)$, meaning that the surface becomes a thin jet at distances from the apparent apex not much larger than the size of the hydrodynamic region R_h, and that the electric field at the surface increases as the jet gets thinner. A consequence of these results is that the effect of the surface tension becomes formally negligible in the jet, when $r_s \ll R_h=O(Q^{1/2})$, because the surface curvature increases less rapidly than the pressure and viscous stresses: $(1/r_s)/(v/x)\sim r_s/Q^{1/2}\ll 1$ in Eq. (6), from the estimates given above.

4. Ion evaporation region

If the estimates of the preceding section are extended down to values of r_s for which $E_n=O(E^*)$, they give $r_s=O(Q^{1/4}/E^*)$ and $v=O(Q^{1/2}E^{*2})$ in the evaporation region. In the absence of space charge effects, the current that evaporates from this region is determined by the rate at which current can be transported in the jet. The maximum possible axial field in the liquid is of the order of $Q^{-1/4}$, assuming that the field induced by the meniscus finally enters the liquid, which along with the estimate of r_s above gives a conduction current of the order of $I=O(E_t r_s^2)=O(Q^{1/4}/E^{*2})$. The surface current, which will be partially convected by the flow beyond the evaporation region, may also be estimated taking $\sigma=O(E^*)$. This gives $\tilde{I}=O(Q^{3/4}E^{*2})$, which is small compared with I when $Q\ll 1/E^{*8}$, in which case most of the current evaporates from the surface.

The flow rate accompanying ion evaporation is nearly ζI in these conditions [see Eqs. (9) and (13)]. It becomes of the order of the injected flow rate when Q decreases to values of the order of $Q_1=\zeta^{4/3}/E^{*8/3}$, but this is typically small compared with the minimum flow rate estimated in the following paragraph. The result suggests that, contrarily to what happens with the electric current, most of the injected flow rate is carried by the spray of drops into which the jet eventually breaks.

Since $\nabla\cdot \boldsymbol{E}^i=0$ in a liquid of constant conductivity, the axial variation of E_t leads to a radial field $E_r^i=O(r_s E_t/x)$ at the liquid side of the surface. The condition that $\beta E_r^i \lesssim E^*$ in the evaporation region [a consequence of the second condition (9), as was discussed before] requires then $Q\gtrsim Q_m=\beta^2/E^{*4}$, which is a condition of consistency of the estimations given above. The order of this minimum flow rate coincides with the estimate of Q^* in (19) for the case $\beta^{1/2}E^*\gg 1$, which means that ion evaporation in the regime analyzed here should occur only in a narrow range of flow rates in this case. In the opposite case of $\beta^{1/2}E^*\ll 1$, however, ion evaporation should be expected over the wider range of flow rates $\beta^2/E^{*4}\lesssim Q\lesssim 1/E^{*8}$.

The pressure variation along the jet can be best estimated from the axial component of the momentum equation in (4) integrated across the jet. Upon using Eq. (7) and then neglecting the radial variations of the pressure and the velocity, this equation yields

$$\pi r_s^2\frac{d}{dx}\left(-p+2\frac{dv}{dx}\right)+2\pi r_s\sigma E_t+6\pi v r_s\frac{dr_s}{dx}=0,$$

$$\text{where}\quad v=\frac{Q}{\pi r_s^2}. \tag{22}$$

The second term of Eq. (22) comes from the electric shear at the surface. The mismatch between this term and the terms proportional to v is the cause of the pressure variation, which has its origin in the vorticity generated at the curved surface. Both effects matter and give rise to pressure variations and normal viscous stresses of the order of E^* in the evaporation region.

5. Jet beyond the evaporation region

The electric shear keeps acting on the jet beyond the evaporation region, where it leads to pressure variations and normal viscous stresses large compared with the normal electric stress. Then the following conditions hold

$$r_s^2\frac{p}{x}\sim r_s^2\frac{v}{x^2}\sim r_s\sigma E_t,\quad v r_s^2\sim Q,\quad \sigma v r_s\sim\tilde{I}, \tag{23}$$

which express the balance of all the terms of Eq. (22) and the conservation of mass and electric current in the jet. From these conditions,

$$r_s=O\left(\frac{Q^{5/8}}{E^* x^{3/4}}\right),\quad \sigma=O\left(\frac{E^*Q^{3/8}}{x^{3/4}}\right),$$

$$p=O\left(\frac{v}{x}\right)=O\left(\frac{E^{*2}x^{1/2}}{Q^{1/4}}\right), \tag{24}$$

where use has been made of the estimate of $\tilde{I}$ given above. Surface tension comes back into play when $1/r_s\sim p$, which happens for $x=O(E^{*4}Q^{3/2})$, and the solution takes the asymptotic form (13) for $x\gg E^{*4}Q^{3/2}$.

IV. DISCUSSION

Values of $\beta^{1/2}E^*$ for formamide and $EMIBF_4$ are of the order of unity, which places these liquids midway between the extreme cases mentioned in (19). Therefore, ions and drops should be expected to coexist in a moderate range of nondimensional flow rates, which is in agreement with experimental results [13–15]. Ion evaporation from the region of high electric field at the beginning of the jet ceases when

the flow rate increases above a value of $O(Q^*)$, whereas a stationary solution of the type discussed here fails to exist below a flow rate of $O(Q_m)$.

The ratio Q_1/Q_m is small for formamide and $EMIBF_4$, which means that the minimum flow rate is attained when the evaporation flow rate is still negligible. The estimates of Sec. III B do not predict a continuous transition to a pure ionic regime through a branch of stationary solutions, which is also in line with the experimental findings of Romero *et al.* [15]. These authors have put forward an explanation of the transition from the drops-and-ions regime to a pure ionic regime. In their scenario, drops come to be shed directly from the evaporation region with nearly constant size and charge but with a frequency that decreases with decreasing Q, until drop ejection vanishes at a certain critical flow rate. Below this flow rate, a pure ionic regime is left, with ion evaporation occurring at a stationary jetlike protrusion of the meniscus that resembles the cusp of a LMIS—though important differences between LMIS and the present ion sources have been already pointed out for the relatively high flow rates of the drops-and-ions regime.

At first sight, the conditions that led to the estimates (20) and (21) are also applicable to the cusp of a pure ionic emitter, but then the additional condition $Q=\zeta I$ should be satisfied because there is no jet that could take care of any remaining flow rate or current. The extra condition is incompatible with the estimate $I=O(Q^{1/4}/E^{*2})$ for all but a particular flow rate, which in any case would be smaller than Q_m. Such negative results suggest that the pure ionic regime is quite different from the regime discussed in this paper.

It has been mentioned before that currents branching off the square root law more abruptly than in Figs. 2 and 3 would probably be obtained if A were increased to more realistic values. This would make the numerical results more similar to the experimental data in Refs. [13,15]. However, a continued exponential increase of the current with decreasing flow rate cannot occur in the framework of the present model, irrespective of the value of A. Though the exponential ion evaporation law in Eq. (8) implies that the ionic current increases very rapidly when the surface electric field rises above E^*, this current has to reach the evaporation region of the surface by conduction in the liquid, which is the current limiting factor in the conditions envisaged here. Conduction is already at about its maximum when evaporation begins [6], and it could increase exponentially only if the electric field in the liquid increased exponentially, which is not the case. In these conditions, the maximum surface field has to adjust itself when the flow rate is decreased so as to remain within a range of $O(1/AE^{*1/2})$ around E^*.

An electric current varying proportionally to $Q^{1/4}$ is marginally observable around the smallest flow rate of Fig. 2, though the flow rates at which evaporation occurs in these computations are substantially smaller than in real experiments and the asymptotic estimates should not be expected to apply very well. The reason is that the value of E^* that has been used in the computations is slightly larger than it is in reality, and Q^* in (19) depends strongly on E^*. Solutions for larger flow rates would have been much more difficult to compute, while the computed solutions already display some of the expected features of real cases.

Figure 6 shows that the surface tension is important everywhere. Surface tension is needed in the upstream conical meniscus to balance the normal electric stress, and in the downstream jet to balance the electric shear-induced pressure. But it should be playing a secondary role in a central region in between, where pressure, viscous, and electric stresses dominate, according to the estimates of Sec. III B 2 for large flow rates. The numerical results show, on the other hand, that the relative importance of pressure and normal viscous stress increases with Q, but they do not overcome surface tension even at the largest flow rates for which a solution has been computed. That the pressure and normal viscous stress have opposite signs in the central region is in agreement with the condition expressed in (24), that they should balance each other when they eventually dominate, but it makes their combined contribution even smaller in the numerical results.

Apart from the obvious reason that the flow rates in the computations are too small for the asymptotic results to be applicable, the persistence of surface tension may be pointing out that pressure and viscous stresses are smaller than in the estimates of Sec. III B 3 that led to (21). The flow is somehow able to negotiate the cone-to-jet transition generating little vorticity and small viscous stresses. The scale v/x for the pressure and viscous stresses is expected to be correct, but the numerical values of both scaled quantities may be small. This result lends support to the proposal of Fernández de la Mora and Loscertales [3], that the cone-to-jet transition should take place in the relaxation region of size $R_e=O(\beta Q)^{1/3}$, despite the fact that the normal viscous stress at the surface in such a region would be much larger than the surface tension when $Q \gg \beta^2$.

The condition $Q \gg \beta^2$, leading to a hydrodynamic region large compared with the relaxation region, is satisfied for the flow rates typical of the drops-and-ions regime, but probably not in the pure ionic regime. It is also not satisfied in the computations summarized in Fig. 2, which detracts from their faithfulness but at the same time may be allowing them to hint at an important feature perhaps to be expected of the pure ionic regime. Namely, the hydrostatic balance of surface tension and normal electric stress extends through the transition region and into the jet, until the electric shear-induced pressure takes over when the normal electric stress declines. Inspection of the numerical results shows that it is the last term of Eq. (6), due to the field tangent to the surface, that contributes most to the normal electric stress when the surface departs from a cone.

V. CONCLUSIONS

Numerical computations and order-of-magnitude estimations have been used to analyze the field-induced evaporation of ions from the surface of a polar liquid in the high-field cone-to-jet transition region of an electrospray. The following results are obtained, all of them in agreement with recent experimental and theoretical results of Fernández de la Mora and co-workers [13,15]. A regime of coexistence of

ions and charged drops exists in a range of flow rates bounded above by the onset of ion evaporation and below by a minimum flow rate below which no stationary solution seems to exist. The total electric current, which is limited by conduction in the liquid, is larger than in the absence of evaporation. When the flow rate is decreased within the range of the drops-and-ions regime, ion evaporation takes care of most of the electric current while most of the injected mass still goes into the drops. No continuous transition to a pure ionic regime is found when the flow rate is further decreased.

An apparently consistent asymptotic structure of the solution in the drops-and-ions regime is proposed. Order of magnitude estimates of the ions and drops contributions to the current are worked out, as well as estimates of the maximum and minimum flow rates bounding this regime.

ACKNOWLEDGMENTS

I am indebted to Professor J. Fernández de la Mora for introducing me to this problem and for useful discussions. This work was supported by the Spanish Ministerio de Ciencia y Tecnología project BFM2002-3860-C02-02.

[1] M. Cloupeau and B. Prunet-Foch, J. Electrost. **25**, 165 (1990).
[2] G.I. Taylor, Proc. R. Soc. A **280**, 383 (1964).
[3] J. Fernández de la Mora and I.G. Loscertales, J. Fluid Mech. **260**, 155 (1994).
[4] A.M. Gañán, J. Dávila, and A. Barrero, J. Aerosol Sci. **28**, 249 (1997).
[5] M. Gamero-Castaño and V. Hruby, J. Fluid Mech. **459**, 245 (2002).
[6] F.J. Higuera, J. Fluid Mech. **484**, 303 (2003).
[7] P. D. Prewett and G.L.R. Mair, *Focussed Ion Beams from LMIS* (Wiley, New York, 1991).
[8] J.V. Iribarne and B.A. Thomsom, J. Chem. Phys. **64**, 2287 (1976).
[9] J.B. Fenn, M. Mann, C.K. Meng, S.F. Wong, and C.M. Whitehouse, Science **246**, 64 (1989).
[10] I.G. Loscertales and J. Fernández de la Mora, J. Chem. Phys. **103**, 5041 (1995).
[11] M. Gamero-Castaño and J. Fernández de la Mora, J. Mass Spectrom. **35**, 790 (2000).
[12] P. Kebarle, J. Mass. Spectrom. **35**, 804 (2000).
[13] M. Gamero-Castaño and J. Fernández de la Mora, J. Chem. Phys. **113**, 815 (2000).
[14] M. Gamero-Castaño, Phys. Rev. Lett. **89**, 147602 (2002).
[15] I. Romero, R. Bocanegra, J. Fernández de la Mora, and M. Gamero-Castaño, J. Appl. Phys. (to be published).
[16] M. Martínez-Sánchez, J. Fernández de la Mora, V. Hruby, M. Gamero-Castaño, and V. Khayms, in *26th International Electric Propulsion Conference*, edited by T. Fujiwara (Kitakyushu, Japan, 1999).
[17] M. Gamero-Castaño and V. Hruby, J. Propul. Power **17**, 165 (2001).
[18] R. Bocanegra, J. Fernández de la Mora, and M. Gamero-Castaño, J. Propul Power (unpublished).
[19] R.G. Forbes, Vacuum **48**, 85 (1997).
[20] D.A. Saville, Annu. Rev. Fluid Mech. **29**, 27 (1997).
[21] L.D. Landau and E.M. Lifshitz, *Electrodynamics of Continuous Media* (Pergamon, Oxford, 1960).
[22] A. Barrero, A.M. Gañán, J. Dávila, A. Palacios, and E. Gómez-González, J. Electrost. **47**, 13 (1999).
[23] F.A. Williams, Proc. Combust. Inst. **24**, 1 (1992); P. Clavin, Annu. Rev. Fluid Mech. **26**, 321 (1994).
[24] V.V. Vladimirov and V.N. Gorshkov, Appl. Phys. A **46**, 131 (1988).
[25] H. Ashley and M. Landahl, *Aerodynamics of Wings and Bodies* (Addison-Wesley, Reading, 1965).